Developmental Cell
Article

Control of Seed Germination by Light-Induced Histone Arginine Demethylation Activity

Jung-Nam Cho,[1] Jee-Youn Ryu,[1,6] Young-Min Jeong,[1,4] Jihye Park,[5] Ji-Joon Song,[5] Richard M. Amasino,[4] Bosl Noh,[1,2,*] and Yoo-Sun Noh[1,3,*]
[1]School of Biological Sciences
[2]Research Institute of Basic Sciences
[3]Plant Genomics and Breeding Institute
Seoul National University, Seoul 151-747, Korea
[4]Department of Biochemistry, University of Wisconsin, Madison, WI 53706, USA
[5]Department of Biological Sciences, Graduate School of Nanoscience and Technology (World Class University), Korea Advanced Institute of Science and Technology, Daejeon 305-701, Korea
[6]Present address: Korea Ocean Research and Development Institute, Ansan 426-744, Korea
*Correspondence: bnoh2003@yahoo.co.kr (B.N.), ysnoh@snu.ac.kr (Y.-S.N.)
DOI 10.1016/j.devcel.2012.01.024

SUMMARY

For optimal survival, various environmental and endogenous factors should be monitored to determine the appropriate timing for seed germination. Light is a major environmental factor affecting seed germination, which is perceived by phytochromes. The light-dependent activation of phytochrome B (PHYB) modulates abscisic acid and gibberellic acid signaling and metabolism. Thus far, several negative regulators of seed germination that act when PHYB is inactive have been reported. However, neither positive regulators of seed germination downstream of PHYB nor a direct mechanism for regulation of the hormone levels has been elucidated. Here, we show that the histone arginine demethylases, JMJ20 and JMJ22, act redundantly as positive regulators of seed germination. When PHYB is inactive, *JMJ20/JMJ22* are directly repressed by the zinc-finger protein SOMNUS. However, upon PHYB activation, *JMJ20/JMJ22* are derepressed, resulting in increased gibberellic acid levels through the removal of repressive histone arginine methylations at *GA3ox1/GA3ox2*, which in turn promotes seed germination.

INTRODUCTION

At maturity, plant embryos cease growth and enter a quiescent state until the environment is favorable for the germination and growth. Several environmental factors, such as light, moisture, and temperature, are known to have profound effects on seed germination. The effect of light on seed germination has been well studied. Since Borthwick et al. (1952) reported the photoreversible, light quality-dependent germination of lettuce seeds, much progress has been made in understanding how the light signal is perceived and transduced to downstream signaling during seed germination. Briefly, photoreversible seed germination is mediated mainly by phytochrome B (PHYB; Shinomura et al., 1994), and the levels of abscisic acid (ABA) and gibberellic acid (GA), which antagonistically regulate seed germination, are oppositely modulated in a light-dependent manner (Seo et al., 2006; Toyomasu et al., 1998; Yamaguchi et al., 1998).

ABA helps to establish and maintain the dormant seed state, and thus inhibits seed germination (Koornneef et al., 2002). Phytochrome activation by light decreases the ABA content of seeds. Consistent with the change in ABA levels, the expression of genes encoding ABA metabolic enzymes changes when phytochrome is activated (Seo et al., 2006). When phytochrome is activated, the ABA anabolic genes, *ABA-DEFICIENT 1* (*ABA1*), *NINE-CIS-EPOXYCAROTENOID DEOXYGENASE 6* (*NCED6*), and *NCED9*, are repressed, whereas an ABA catabolic gene, *CYP707A2*, which encodes an ABA 8′-hydroxylase, is upregulated (Kim et al., 2008; Oh et al., 2007). Therefore, the differential expression of genes encoding ABA metabolic enzymes contributes to a decrease in ABA content and the resulting promotion of seed germination upon light exposure. In addition to the light regulation of ABA metabolic genes, the transcription of the ABA signaling gene *ABA INSENSITIVE 3* (*ABI3*) is also affected by mutations in *PHYB* in *Arabidopsis* seedlings (Mazzella et al., 2005). Thus, phytochrome regulates not only the metabolic genes but also the ABA signaling genes.

GA induces seed germination in part via a promotion of cell division and expansion. The light activation of phytochrome increases endogenous GA levels and GA responsiveness by regulating the expression of GA signaling genes in addition to metabolic genes (Seo et al., 2009; Toyomasu et al., 1998). Activated phytochrome increases the expression of GA anabolic genes, namely *GIBBERELLIN 3 β-HYDROXYLASE 1* (*GA3ox1*) and *GA3ox2*, whereas a GA catabolic gene, *GA2ox2*, is repressed upon phytochrome activation (Yamauchi et al., 2007). In addition, *RGA*, *GAI*, and *RGL2*, which encode well-known GA-signaling DELLA proteins that play important roles in seed germination, are also altered in their expression by phytochrome activation (Oh et al., 2007). ABA and GA antagonistically regulate each other in the light-dependent seed germination pathway. For example, mutations in the ABA metabolic genes, *CYP707A2* and *ABA2*, change the mRNA levels of *GA3ox1* and *GA3ox2* in *Arabidopsis* seeds (Seo et al., 2006). On the other hand, the

expression of ABA metabolic genes is altered in GA-deficient mutants or when exogenous GA is applied (Oh et al., 2007).

Several transcription factors have been reported to regulate light-dependent seed germination. A basic helix-loop-helix (bHLH) protein, PHYTOCHROME-INTERACTING FACTOR 3-LIKE 5 (PIL5), represses seed germination during the dark period (Oh et al., 2004). Light-activated phytochrome translocates to the nucleus and degrades PIL5 protein via the ubiquitin-proteasome system (Oh et al., 2006). PIL5 directly upregulates the expression of the zinc-finger protein SOMNUS (SOM), another important repressor of seed germination, in concert with ABI3 (Park et al., 2011; Kim et al., 2008). It was recently reported that DOF AFFECTING GERMINATION 1 (DAG1) also represses seed germination downstream of PIL5 by directly repressing *GA3ox1*, but not *GA3ox2* (Gabriele et al., 2010). The PHYB-PIL5-SOM pathway might be the major controller of light-dependent seed germination, and consistent with this model, a number of hormone-related genes are regulated by PIL5 and SOM (Oh et al., 2009; Kim et al., 2008). Although the role of PIL5 on SOM is through direct transcriptional activation (Kim et al., 2008), to our knowledge, it is not known how SOM affects the expression of hormone-related genes.

Gene transcription can be activated or repressed by post-translational histone methylation depending on which lysine or arginine residues are methylated (Li et al., 2007). Lysine and arginine histone methylation are catalyzed by two distinct families of enzymes: the SET domain-containing proteins (Kouzarides, 2007) and protein arginine methyltransferase (PRMT) family proteins (Di Lorenzo and Bedford, 2011), respectively. Numerous recent studies have shown that these histone methylations can also be removed by at least two distinct classes of enzymes, including the Lysine-Specific Demethylase 1 class of proteins and the Jumonji C (JmjC) domain-containing proteins (reviewed in Pedersen and Helin, 2010). The human JmjC domain-containing protein, JMJD6, has been reported to demethylate both asymmetrically and symmetrically dimethylated H3 arginine 2 (H3R2me2) and H4 arginine 3 (H4R3me2; Chang et al., 2007). However, this activity was questioned by another study reporting that JMJD6 has lysyl hydroxylation activity toward the splicing factor U2AF2 (Webby et al., 2009). Because the levels of H3R2me2 and H4R3me2 are known to be negatively correlated with the level of trimethylated H3 lysine 4 (H3K4me3; Guccione et al., 2007; Hyllus et al., 2007), a well-known epigenetic marker reflecting transcriptional activity, high levels of H3R2me2 and H4R3me2 are thought to cause transcriptional repression. Although the biological functions of histone lysine demethylases have been extensively studied in many eukaryotic organisms, the in vivo roles of histone arginine (HR) demethylases have not yet been carefully explored. Here, we report evidence that implicates light-induced HR demethylation in *Arabidopsis* seed germination.

RESULTS

Loss of Both *JMJ20* and *JMJ22* Leads to a Reduction in Seed Germination Efficiency during PHYB Activation

Our previous reports have demonstrated that some *Arabidopsis* JmjC domain proteins possess the expected target specificities based on sequence similarities of their JmjC domains with known JmjC proteins (Ko et al., 2010; Jeong et al., 2009). To identify putative HR demethylases among the 21 JmjC domain-containing proteins of *Arabidopsis thaliana* (JMJs or AtJmjs; Hong et al., 2009; Hahn et al., 2008), we searched for sequence similarity within their JmjC domains to the JmjC domain of human JMJD6, a known HR demethylase (Chang et al., 2007). Analysis of the amino acid sequences of the 21 JMJ proteins revealed that three of the JMJ proteins, JMJ20 (AtJmj13 and At5g63080), JMJ21 (AtJmj10 and At1g78280), and JMJ22 (AtJmj11 and At5g06550), were most similar to JMJD6 (see Figure S1 available online).

To examine the biological functions of *JMJ20*, *JMJ21*, and *JMJ22*, we obtained T-DNA insertion mutants of *JMJ20* (*jmj20-1*) and *JMJ22* (*jmj22-1*) (Figure 1A), but we could not obtain homozygous mutants for *JMJ21*. *jmj20-1* and *jmj22-1* are likely to be loss-of-function null alleles because the full-length *JMJ20* and *JMJ22* transcripts were not detected in the corresponding homozygous mutants (Figure S1C). Considering the high sequence similarity and possible functional redundancy between JMJ20 and JMJ22 (Figure S1), we also generated *jmj20-1 jmj22-1* double mutants, and then performed a variety of phenotypic assays on the single and double mutants. Although these mutants displayed wild-type (WT) phenotypes throughout vegetative development under regular growth conditions (Figure S1D), the double-mutant seeds showed a reduced germination efficiency after a red light (R)-pulse treatment (Figure 1B). For this experiment, we grew WT and mutant plants side by side, and their harvested seeds were stored dry at room temperature for more than 2 months to achieve full after ripening before being subjected to R-pulse experiments, which assess PHYB-dependent germination. The reduced germination efficiency of the double-mutant seeds was not likely to have resulted from a defect in seed development because the seeds of the double mutants were morphologically indistinguishable from those of WT (Figure S1E).

To confirm that the lower germination efficiency of the double-mutant seeds was caused by the mutations in *JMJ20* and *JMJ22*, we attempted to rescue the mutant phenotype with translational β-glucuronidase (GUS) fusion constructs containing the native promoters and genomic coding regions of *JMJ20* and *JMJ22*. Each construct (*JMJ20:GUS* or *JMJ22:GUS*) was introduced into the double mutants by *Agrobacterium*-mediated transformation, and two representative transgenic lines, containing *JMJ20:GUS* or *JMJ22:GUS*, were investigated for their seed germination efficiency under PHYB-dependent germination conditions. Figure 1C shows that the introduction of *JMJ20:GUS* or *JMJ22:GUS* completely rescued the reduced germination efficiency of the double mutants and demonstrates that the defect is caused by lesions in *JMJ20* and *JMJ22*. This result indicates that these two related genes have redundant roles in promoting seed germination.

Because longer exposure of R results in a higher germination rate by increasing the endogenous levels of GA (Oh et al., 2006), we examined the germination efficiency of the double-mutant seeds treated with R for different durations. As shown in Figure 1D, the double-mutant seeds showed a lower germination rate when treated with 1 or 5 min of R compared with the seeds of WT and each single mutant. However, the germination rate of the double-mutant seeds was indistinguishable from WT and each single mutant after 60 min of R exposure. Application of

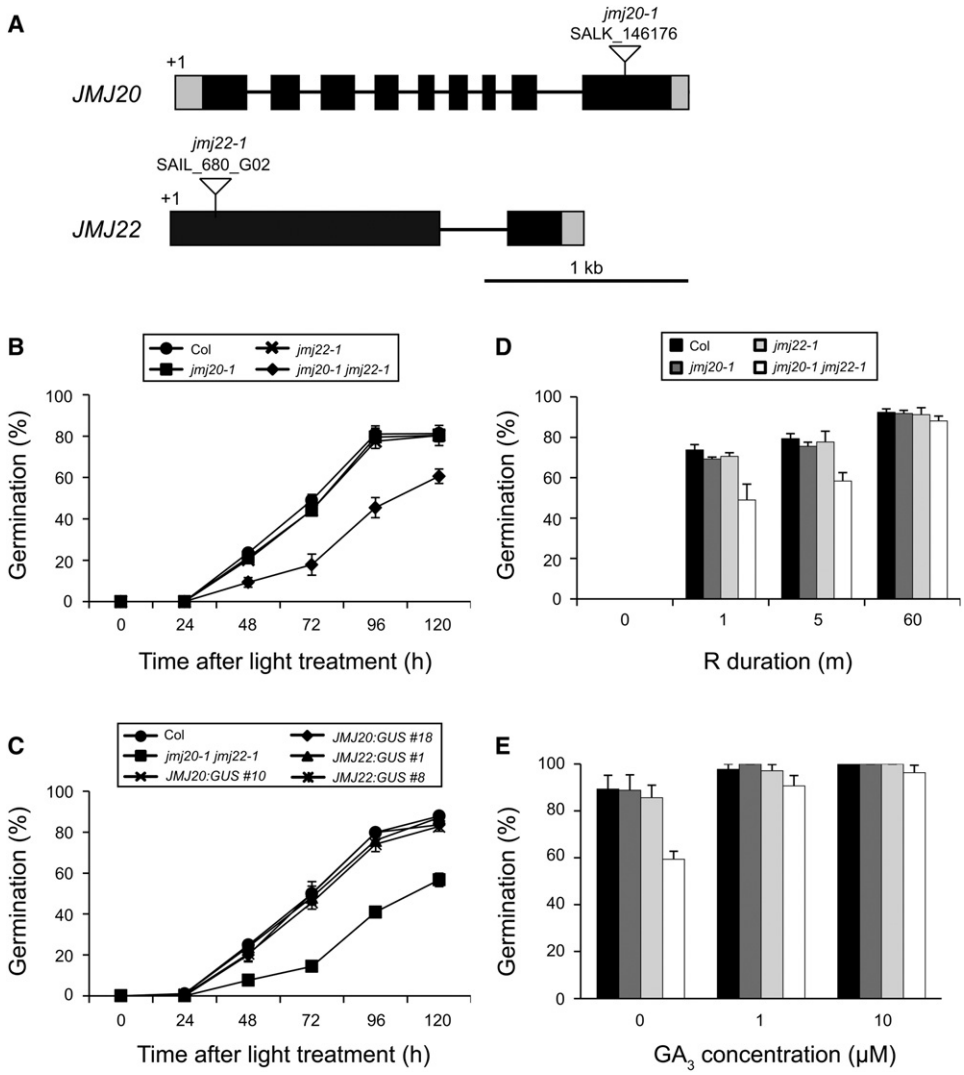

Figure 1. Germination Efficiency Is Reduced in *jmj20 jmj22* Double-Mutant Seeds

(A) The gene structures of *JMJ20* and *JMJ22*. Black boxes are exons, and gray boxes are untranslated regions (UTRs). Intergenic regions or introns are marked with lines. The transcription start site is indicated by +1, and the T-DNA insertion site in each mutant allele is marked with triangle.

(B) The PHYB-dependent germination assay. WT, single, and double-mutant seeds were imbibed for 1 hr (h) in the dark. Then, the seeds were exposed to 5 min of a R pulse immediately after 5 min of a FR pulse (B, C, and E). Light-treated seeds were incubated in the dark, and germinated seeds were counted every 24 hr (B and C). Error bars represent SD in (B)–(E). Col, Columbia-0 WT.

(C) Complementation of the defective germination phenotype of *jmj20 jmj22* by *JMJ20:GUS* or *JMJ22:GUS*. Two representative transgenic lines of *JMJ20:GUS* or *JMJ22:GUS* introduced into *jmj20-1 jmj22-1* were used for the PHYB-dependent germination assay.

(D) The PHYB-dependent germination assay with different R durations. Seeds were exposed to R for the indicated time period (m, min) after 5 min of FR pulse. Results shown are the percentage of germinated seeds at 5 days after light treatment (D and E).

(E) The PHYB-dependent germination assay with exogenous GA_3. The indicated amount of GA_3 was added to the germination media.

See also Figure S1.

1 and 10 μM of exogenous GA to the double-mutant seeds also partially and fully rescued the germination defect, respectively (Figure 1E). In summary, the data collectively indicate that the reduced germination rate of the double-mutant seeds is likely to be caused by lower endogenous GA levels.

JMJ20 and JMJ22 Expression in Embryos and Their Nuclear Localization

Because *JMJ20* and *JMJ22* have roles in the light-dependent germination pathway, we studied the spatial expression patterns of *JMJ20* and *JMJ22* in far-red light (FR)- and R-treated embryos. We performed histochemical GUS staining of the functional JMJ20:GUS and JMJ22:GUS fusion proteins discussed above (Figure 1C). As shown in Figure 2A, in FR-treated *JMJ22:GUS* seeds, staining was observed mainly in the radicle of the embryo. Interestingly, GUS activity was higher after R treatment, and the expression domain of JMJ22:GUS spread to the cotyledons. The GUS activity of JMJ20:GUS was detected in the entire region of the embryo in FR-treated seeds and appeared to increase after R treatment as with JMJ22:GUS

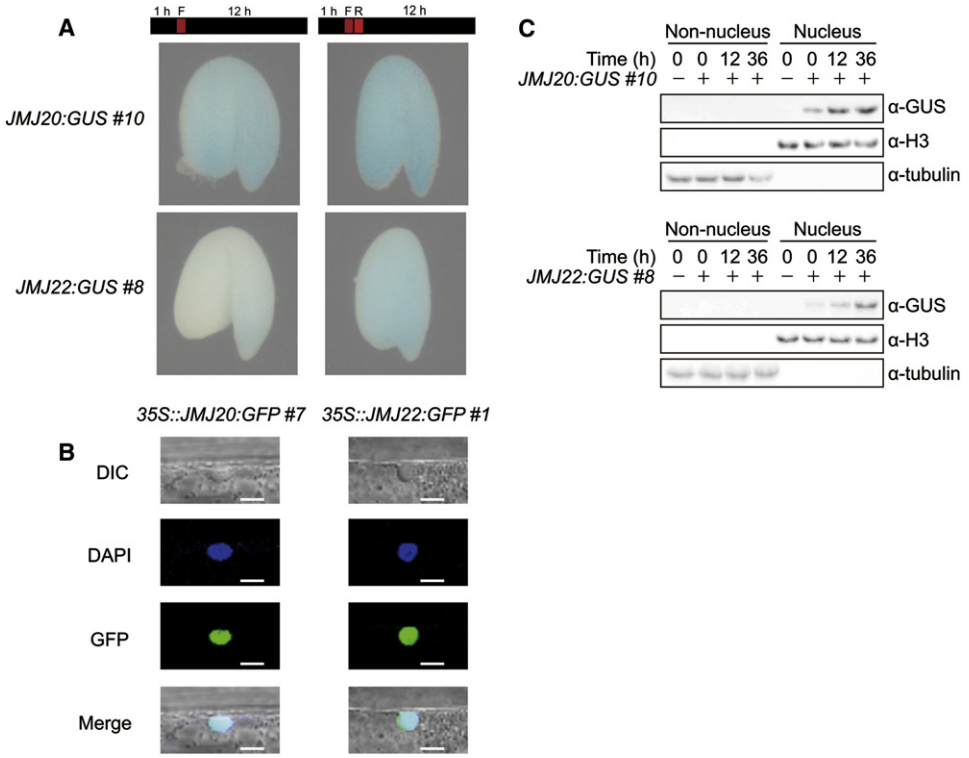

Figure 2. The Expression of JMJ20 and JMJ22 in the Embryo and Their Nuclear Localization

(A) The spatial expression pattern of JMJ20:GUS and JMJ22:GUS in the embryo. FR (F)- and R (R)-treated seeds were fixed and dissected. The light treatment regime (5 min each for F and R) is indicated in the diagram at the top. Black boxes indicate dark incubation periods. Rescued embryos were analyzed for GUS expression.

(B) Nuclear localization of JMJ20:GFP and JMJ22:GFP. Roots of 10-day-old long-day (LD) grown *35S::JMJ20:GFP* and *35S::JMJ22:GFP* transgenic plants were analyzed for subcellular localization using a confocal fluorescence microscope. DAPI was used to stain the nucleus. From the top, differential interference contrast (DIC), DAPI, GFP, and merged images from the three above are presented. Scale bars represent 10 μm.

(C) Nuclear localization and R induction of JMJ20:GUS and JMJ22:GUS. Nuclear and nonnuclear proteins were fractionated from *JMJ20:GUS*-, *JMJ22:GUS*-containing transgenic (+), or *jmj20-1 jmj22-1* (−) seeds incubated in the dark for 0, 12, or 36 hr after 5 min R treatment and subjected to western blot analyses using anti-GUS antibody. H3 and tubulin were detected as nuclear and nonnuclear protein controls, respectively.

See also Figure S2.

(Figure 2A). Previous reports have shown that *GA3ox1* and *GA3ox2* are expressed mainly in the embryonic axis (Ogawa et al., 2003). Thus, our study shows that *JMJ20* and *JMJ22* are expressed in the embryonic regions where *GA3ox1* and *GA3ox2* are also expressed, although the expression domains of these *JMJ* genes are not identical to the expression domain of the GA anabolic genes.

Because JMJ20 and JMJ22 are predicted to act as HR demethylases, we suspected that these proteins might be localized to the nucleus. To test this possibility, we generated a construct producing green fluorescent protein (GFP)-tagged JMJ20 or JMJ22 under the control of the cauliflower mosaic virus (CaMV) 35S promoter. In the roots of transgenic plants containing each construct, JMJ20:GFP and JMJ22:GFP fusion proteins were localized exclusively in nuclei (Figure 2B). We also obtained nuclear and nonnuclear proteins from the R-treated *JMJ20:GUS*- or *JMJ22:GUS*-containing transgenic seeds and analyzed GUS expression by western blot (Figure 2C). Both JMJ20:GUS and JMJ22:GUS were detected only in nuclei, and their levels were increased gradually after R treatment. Consistent with the induction at protein level, the mRNA levels of *JMJ20* and *JMJ22* were also increased after R treatment as the mRNA levels of *GA3ox1* and *GA3ox2* (Figure S2). However, unlike *JMJ20*/*JMJ22*, the mRNA expression of *JMJ21* in seeds was not induced by R (Figure S2), suggesting that *JMJ21* might not have a redundant role with *JMJ20*/*JMJ22* in light-dependent seed germination. In sum, the results above indicate that JMJ20 and JMJ22 are R-induced nuclear proteins, consistent with their possible role as histone modifiers acting in light-dependent germination.

Downregulation of *GA3ox1* and *GA3ox2* Is Associated with a Reduced Germination Efficiency in *jmj20 jmj22*

Light-dependent seed germination is largely regulated by two phytohormones: ABA and GA. As mentioned in the Introduction, a number of studies have revealed that light activation of phytochrome modulates the expression of genes encoding enzymes with roles in the synthesis or catabolism of these two hormones. ABA and GA signaling factors are also important in the regulation of seed germination (Seo et al., 2009; Oh et al., 2007). In addition, it was recently reported that transcription factors that act as repressors of seed germination, such as PIL5, SOM, and

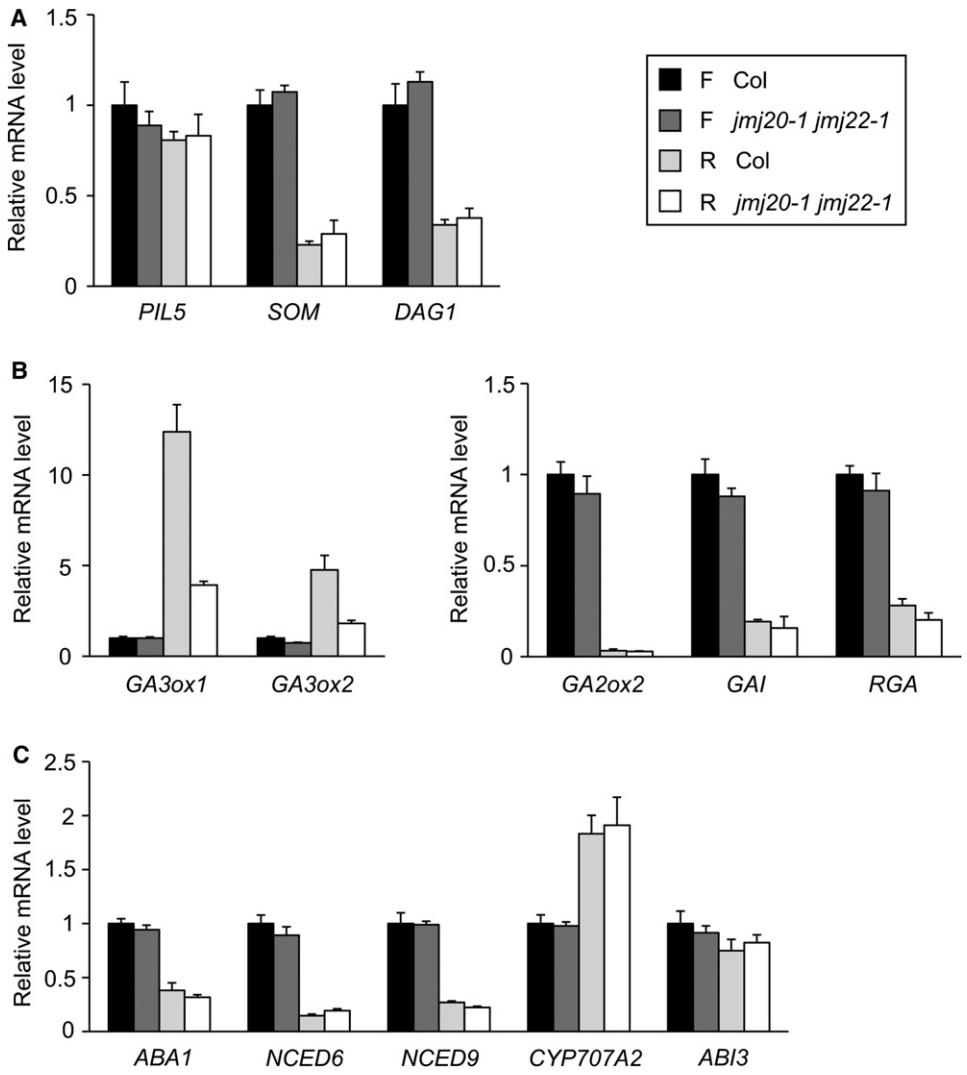

Figure 3. The Expression of *GA3ox1* and *GA3ox2* Is Reduced in *jmj20 jmj22* Double Mutants

(A) Relative transcript levels of *PIL5*, *SOM*, and *DAG1*, repressors of seed germination that act downstream of PHYB. Transcript levels were analyzed by qRT-PCR using gene-specific primers (Supplemental Experimental Procedures), and the levels in F WT were set to 1 after normalization by *Actin 2* (*ACT2*; A–C). Error bars represent SD in (A)–(C). F, FR treated; R, R treated after FR treatment. See the Supplemental Experimental Procedures for the detail of light treatment.

(B) Relative transcript levels of genes encoding GA metabolic enzymes (*GA3ox1*, *GA3ox2*, and *GA2ox2*) or signaling components (*GAI* and *RGA*).

(C) Relative transcript levels of genes encoding ABA metabolic enzymes (*ABA1*, *NCED6*, *NCED9*, and *CYP707A2*) or signaling component (*ABI3*).

DAG1, seem to mediate the light signal from phytochromes to hormones (Gabriele et al., 2010; Oh et al., 2004, 2009; Kim et al., 2008). Because JMJ20 and JMJ22 might act at the transcriptional level, we tested the effect of *jmj20* and *jmj22* mutations on the steady-state mRNA levels of genes known to have roles in light-dependent germination. Accordingly, RNAs extracted from FR- and R-treated WT and double-mutant seeds were used for reverse transcription followed by quantitative real-time PCR (qRT-PCR) analyses. We observed that mRNA levels of *SOM* and *DAG1*, but not *PIL5*, were downregulated in R-treated WT seeds (Figure 3A), as reported previously (Gabriele et al., 2010; Kim et al., 2008). However, the transcript levels of these genes were not significantly different between WT and double mutants (Figure 3A).

Next, we analyzed the transcript levels of genes related to GA metabolism and signaling (Figure 3B). *GA3ox1* and *GA3ox2* encode β-hydroxylases that convert GA to an active form, whereas *GA2ox2* encodes a GA catabolic enzyme (Williams et al., 1998). Both *RGA* and *GAI* encode GA-signaling DELLA proteins and are direct targets of PIL5 (Oh et al., 2007). The transcript levels of *GA3ox1* and *GA3ox2* were drastically increased by R treatment in WT (Figure 3B). However, the induction of these genes by R was strongly attenuated in *jmj20 jmj22* double mutants. On the other hand, there was no significant difference in the transcript levels of *GA2ox2*, *RGA*, and *GAI* between WT and double mutants before and after R treatment (Figure 3B). ABA-related genes were also analyzed (Figure 3C). *ABA1*, *NCED6*, and *NCED9* are ABA biosynthesis genes, whereas *CYP707A2*

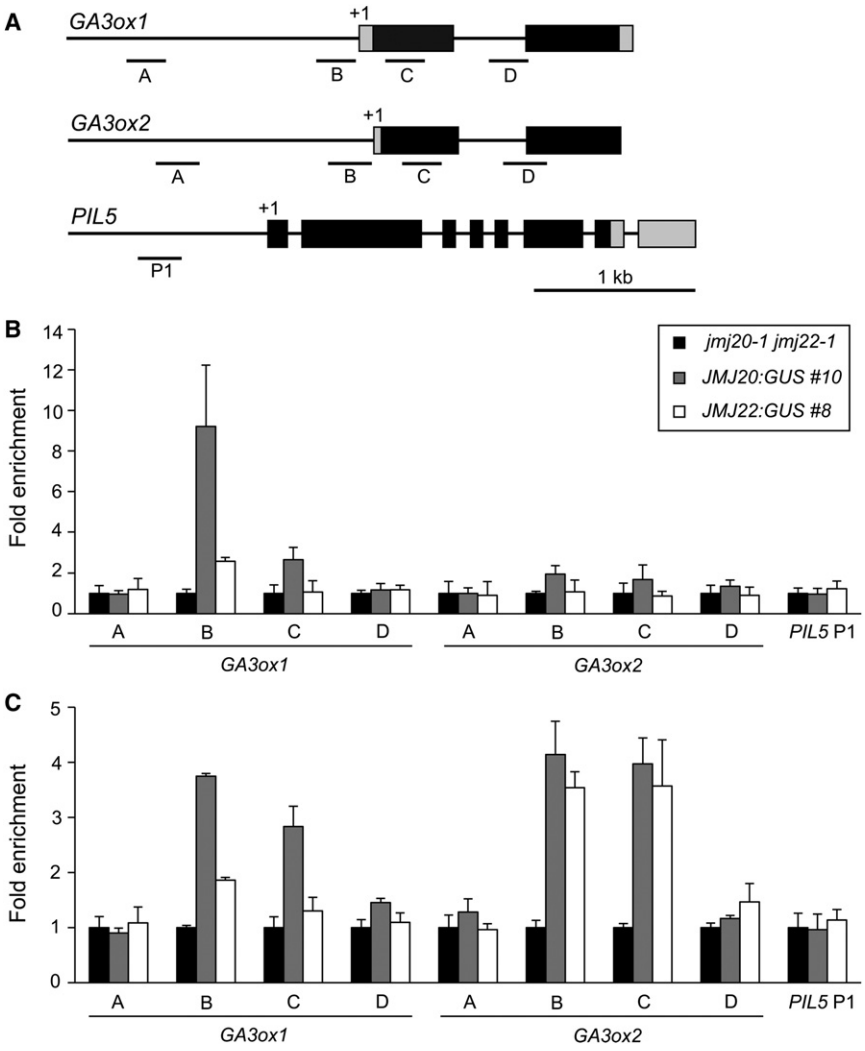

Figure 4. JMJ20:GUS and JMJ22:GUS Directly Bind to the *GA3ox1* and *GA3ox2* Promoters

(A) The gene structures of *GA3ox1*, *GA3ox2*, and *PIL5*, and the regions amplified in quantitative PCR after ChIP. Schematics are as described in Figure 1A.

(B) ChIP-quantitative PCR analyses for the binding of JMJ20:GUS and JMJ22:GUS to *GA3ox1* and *GA3ox2*. Seeds were imbibed for 1 hr, exposed for 5 min to FR followed by 30 min of R exposure, and incubated for 12 hr in the dark. Chromatin isolated from these seeds was immunoprecipitated with an anti-GUS antibody, and the amount of coimmunoprecipitated DNA was measured by quantitative PCR using locus-specific primers (Supplemental Experimental Procedures) for the regions indicated (A). The P1 region of the *PIL5* promoter served as a nonspecific control (B and C). Levels in nontransgenic control (*jmj20-1 jmj22-1*) seeds were set to 1 after normalization to the levels of input DNA (B and C). Error bars represent SD in (B) and (C).

(C) ChIP-quantitative PCR analyses for the binding of JMJ20:GUS and JMJ22:GUS to *GA3ox1* and *GA3ox2*. Experiments were performed as in (B) except that seeds were incubated in the dark for 27 hr instead of 12 hr following R exposure before harvest.

and *ABI3* are ABA catabolic and signaling genes, respectively (Seo et al., 2006, 2009). None of these ABA-related genes was differentially expressed between WT and double mutants before and after R treatment. Thus, we infer that the lower induction of *GA3ox1* and *GA3ox2* after R treatment may result in lower level of endogenous GA and, subsequently, the lower germination efficiency in the *jmj20 jmj22* double mutants compared with WT (Figure 1B). These results are consistent with the fact that exogenous GA treatment could rescue the germination defect in the double mutants (Figure 1E).

Direct Regulation of *GA3ox1* and *GA3ox2* by JMJ20 and JMJ22

Next, we investigated whether the involvement of JMJ20 and JMJ22 in *GA3ox1* and *GA3ox2* expression is direct by performing chromatin immunoprecipitation (ChIP) assays, using the *JMJ20:GUS* and *JMJ22:GUS* transgenic seeds described in Figure 1C. After a 12 hr dark incubation of R-treated seeds, JMJ22:GUS weakly bound to the *GA3ox1*, but not *GA3ox2*, proximal promoter region, whereas JMJ20:GUS showed relatively strong binding to *GA3ox1*, but only weak binding to the *GA3ox2*, region around the transcription start site (Figure 4B). Thus, binding of these fusion proteins to *GA3ox2* was weaker than that of *GA3ox1* after a 12 hr dark incubation for R-treated seeds. A previous (Seo et al., 2006) and our own (Figure S2) studies showed differential expression kinetics between *GA3ox1* and *GA3ox2* after R treatment. In these studies, the expression of *GA3ox1* peaked after a 12 hr incubation, whereas that of *GA3ox2* showed slower kinetics peaking after 36 hr. Therefore, the differential binding of JMJ20:GUS and JMJ22:GUS to these two loci may be because 12 hr of incubation after R treatment is not sufficient for full induction of *GA3ox2*. For this reason, we also performed ChIP after a longer incubation period (27 hr) in the dark (Figure 4C). In this case, the binding of the fusion proteins to *GA3ox2* was as strong as to *GA3ox1*. Moreover, JMJ22:GUS showed a stronger binding to *GA3ox2* than to *GA3ox1*. In summary, the aforementioned results indicate that JMJ20 and JMJ22 directly act on *GA3ox1* and *GA3ox2* chromatin near their transcription start sites, and their binding efficiency correlates with the induction pattern of *GA3ox1* and *GA3ox2*.

The Intrinsic HR Demethylase Activity of JMJ20 and the Effect of JMJ20 and JMJ22 on *GA3ox1* and *GA3ox2* Chromatin

Because both JMJ20 and JMJ22 proteins possess JmjC domains that are similar to the JmjC domain of JMJD6 (Figure S1), a known HR demethylase (Chang et al., 2007), and were shown to directly associate with *GA3ox1* and *GA3ox2*

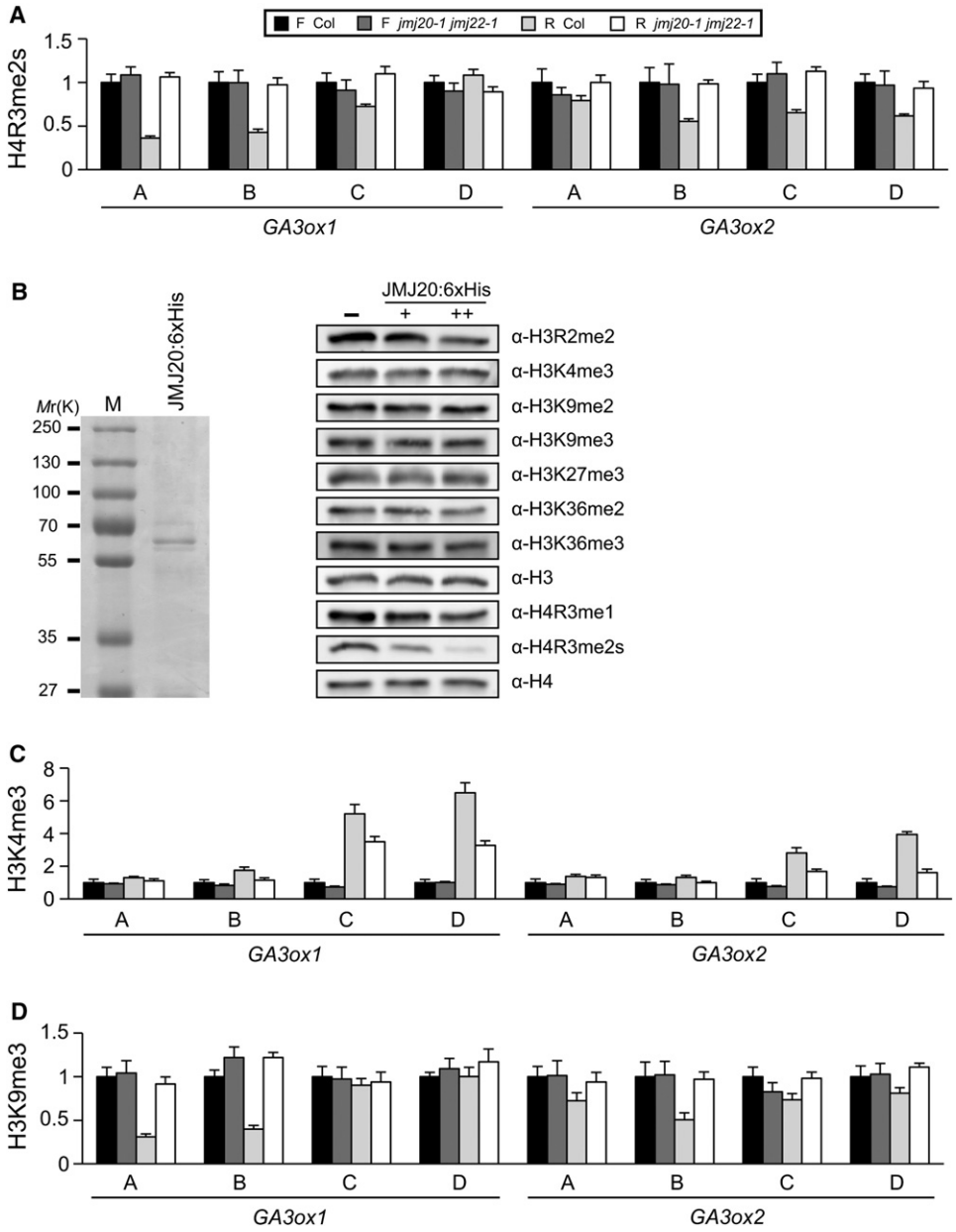

Figure 5. The Intrinsic HR Demethylase Activity of JMJ20 and the Effect of JMJ20 and JMJ22 on *GA3ox1* and *GA3ox2* Chromatin

(A) Relative enrichment of H4R3me2s at *GA3ox1* and *GA3ox2* in WT and *jmj20 jmj22* seeds. FR- and R-treated WT and double-mutant seeds were used for the ChIP assay using the specific antibodies indicated (A, C, and D), and the amount of coimmunoprecipitated DNA was measured by quantitative PCR using locus-specific primers (Supplemental Experimental Procedures) for the *GA3ox1* and *GA3ox2* regions indicated in Figure 4A (A, C, and D). Light treatment was performed as described in Figure 3. Levels in F WT seeds were set to 1 (A, C, and D) after normalization to the level at the *AtMu1* (A and D) or *ACT2* (C) locus. Error bars represent SD in (A), (C), and (D).

(B) Coomassie-stained, purified JMJ20:6×His protein is shown on the left. The in vitro histone demethylase activity assay using calf thymus histone as substrate is shown on the right. The demethylation reaction was performed without (–) or with 1 (+) or 2 (++) μg of purified JMJ20:6×His protein.

(C) The relative enrichment of H3K4me3.

(D) The relative enrichment of H3K9me3.

See also Figure S3.

chromatin (Figure 4), the HR methylation state at *GA3ox1* and *GA3ox2* in WT versus *jmj20 jmj22* double mutants was compared with or without R treatment. In WT, symmetric H4R3me2 (H4R3me2s) levels were reduced in multiple regions of *GA3ox1* and *GA3ox2* following R treatment, but not in the double mutant (Figure 5A). However, H3R2me2 levels were not significantly affected by R both in WT and the double mutant (Figure S3A). These results indicate that JMJ20 and JMJ22 affect the level of

H4R3me2s but not H3R2me2 at *GA3ox1* and *GA3ox2* in vivo in an R-dependent manner during seed germination.

Next, we tested whether JMJ20 and JMJ22 have HR demethylase activity in vitro. Although we could not express the full-length JMJ22 in several expression systems employed, we could express the full-length JMJ20 as a carboxy-terminal 6× histidine-tagged protein (JMJ20:6×His) in *E. coli*. JMJ20:6×His was purified to near homogeneity (Figure 5B, left) and was subjected to an in vitro histone demethylase activity assay. JMJ20:6×His-mediated histone demethylase activity was reflected in the decreased signal on western blots with antibodies specific for methylated H3 or H4 residues (Figure 5B, right). The incubation of the recombinant JMJ20:6×His protein with histone substrates in the demethylase assays resulted in reduced levels of H3R2me2, H4R3me1, and H4R3me2s, but not of H3K4me3, H3K9me2, H3K9me3, H3K27me3, H3K36me2, and H3K36me3 (Figure 5B, right). These results indicate that JMJ20:6×His protein, similarly to human JMJD6 (Chang et al., 2007), possesses intrinsic H3R2- and H4R3-specific demethylase activity that is independent of the state of the methyl group. Thus, the R-dependent decrease in H4R3me2s levels at *GA3ox1* and *GA3ox2* in WT but not *jmj20 jmj22* (Figure 5A) is likely to be directly caused by the H4R3 demethylase activities of JMJ20 and JMJ22. However, regardless of the intrinsic H3R2 demethylase activity of JMJ20, JMJ20 and JMJ22 might not act as H3R2 demethylases in vivo at *GA3ox1* and *GA3ox2* based on the constant H3R2me2 levels at these loci in WT and *jmj20 jmj22* seeds before and after R treatment (Figure S3A).

H4R3me2s contributes to a repressive chromatin state (reviewed in Di Lorenzo and Bedford, 2011), and some crosstalk between H4R3me2s and other histone markers is known (Fischle et al., 2003). For example, crosstalk has been observed in *Arabidopsis* at *FLOWERING LOCUS C* (*FLC*) chromatin; reduced H4R3me2s at *FLC* chromatin due to mutations in *PROTEIN ARGININE METHYLTRANSFERASE 5* (*AtPRMT5*) is associated with lower levels of both H3K9me3 and H3K27me3 (Schmitz et al., 2008). Thus, we measured several histone methylation markers other than H4R3me2s to address if a similar crosstalk is also observed at *GA3ox1* and *GA3ox2*. R treatment caused increased levels of H3K4me3, a representative marker for active chromatin, in the gene bodies of *GA3ox1* and *GA3ox2* in WT seeds, whereas the increase was attenuated in *jmj20 jmj22* double-mutant seeds (Figure 5C). The levels of H3K9me3 were also affected similarly to those of H4R3me2s by R and *jmj20 jmj22* mutations (Figure 5D). However, the levels of H3K27me3, a representative marker of repressive chromatin, were not significantly changed by R treatment or by mutations in *JMJ20* and *JMJ22* (Figure S3B). In sum, at *GA3ox1* and *GA3ox2*, H4R3me2s levels are correlated with the levels of H3K9me3 and H3K4me3 in a positive and negative manner, respectively, but not with H3K27me3 levels. Therefore, the inefficient removal of H4R3me2s/H3K9me3 and reduced accumulation of H3K4me3 in *jmj20 jmj22* double-mutant seeds during R-induced germination is likely to cause hypo-induction of *GA3ox1* and *GA3ox2*, resulting in lower germination efficiency.

SOM Directly Represses *JMJ20* and *JMJ22* Expression

A previous study has shown that PIL5 directly activates the transcription of *SOM*, and both PIL5 and SOM act as upstream repressors of *GA3ox1* and *GA3ox2* in the absence of R (Kim et al., 2008). However, to our knowledge, whether the effect of SOM on *GA3ox1* and *GA3ox2* is direct has not been addressed. Our data show that the expression of *PIL5* and *SOM* is not affected by *jmj20* and *jmj22* mutations (Figure 3A), and JMJ20/JMJ22 proteins act directly on *GA3ox1* and *GA3ox2* chromatin as HR demethylases (Figures 4 and 5). Thus, one possibility is that SOM acts on *GA3ox1* and *GA3ox2* through JMJ20 and JMJ22. To address this possibility, we analyzed the effect of the *pil5-1* and *som-1* mutations on the transcript levels of *JMJ20* and *JMJ22* in FR- and R-treated seeds. Notably, the transcript levels of *JMJ20* and *JMJ22* were greatly increased in *pil5* and *som* mutant seeds under FR (Figures 6A and 6B). Their levels were also increased in WT but not in *phyB* mutant seeds following R treatment, which caused the downregulation of *SOM* (Figures 6A, 6B, and S2). Then, we constitutively expressed *SOM* and evaluated the expression levels of *JMJ20/JMJ22* and *GA3ox1/GA3ox2* under R (i.e., under the condition where intrinsic *SOM* is repressed). The transcript levels of both *JMJ20/JMJ22* and *GA3ox1/GA3ox2* were largely reduced in *35S::SOM:GFP* transgenic seeds (Kim et al., 2008) compared with WT seeds (Figure 6C), indicating that *JMJ20/JMJ22* and *GA3ox1/GA3ox2* can be repressed efficiently even with activated PHYB and PIL5 degradation if SOM is constitutively provided.

Because the data in Figures 6A–6C are consistent with *JMJ20* and *JMJ22* functioning downstream of the PHYB-PIL5-SOM pathway, we examined the epistatic relationship between *PHYB*, *PIL5*, or *SOM* and *JMJ20/JMJ22* by testing the germination efficiency of *phyB jmj20 jmj22*, *pil5 jmj20 jmj22*, and *som jmj20 jmj22* triple mutants under R or FR. *phyB jmj20 jmj22* triple mutants did not germinate like *phyB* single mutants under R, whereas the R-independent germination phenotype of *pil5* mutants was partially suppressed in *pil5 jmj20 jmj22* triple mutants (Figure S4A). Similarly, approximately 80% germination efficiency of *som* mutants under FR was reduced to approximately 50% in *som jmj20 jmj22* triple mutants (Figure 6D). Thus, *JMJ20/JMJ22* are at least partially required for the efficient germination of *pil5* and *som* under FR and act in the PHYB-PIL5-SOM pathway at the downstream of *SOM*. Consistent with the germination efficiency, the derepressed expression of *GA3ox1* and *GA3ox2* in *som* mutants under FR was also attenuated by the *jmj20 jmj22* double mutation (Figure 6E). In sum, the data in Figures 6A–6E indicate that SOM acts as an upstream repressor of *JMJ20* and *JMJ22* under FR.

Next, we examined if the repressive effect of SOM on *JMJ20* and *JMJ22* is direct by performing ChIP assays using transgenic seeds expressing SOM:GFP under the native *SOM* promoter (*pSOM::SOM:GFP*; Park et al., 2011). As shown in Figure 6G, the SOM:GFP fusion protein associated with the distal promoter regions of *JMJ20* and *JMJ22* but not with the promoter region of *PIL5* under FR, and ChIP assays using the *35S::SOM:GFP* transgenic seeds showed similar results (Figure S4B), although yeast one-hybrid assays indicated that SOM alone might not be able to bind to the *JMJ20/JMJ22* promoters (Figure S4C). Thus, *JMJ20* and *JMJ22* appear to be direct repression targets of SOM.

All our data suggested a possibility of enhanced seed germination through the derepression of *GA3ox1* and *GA3ox2*

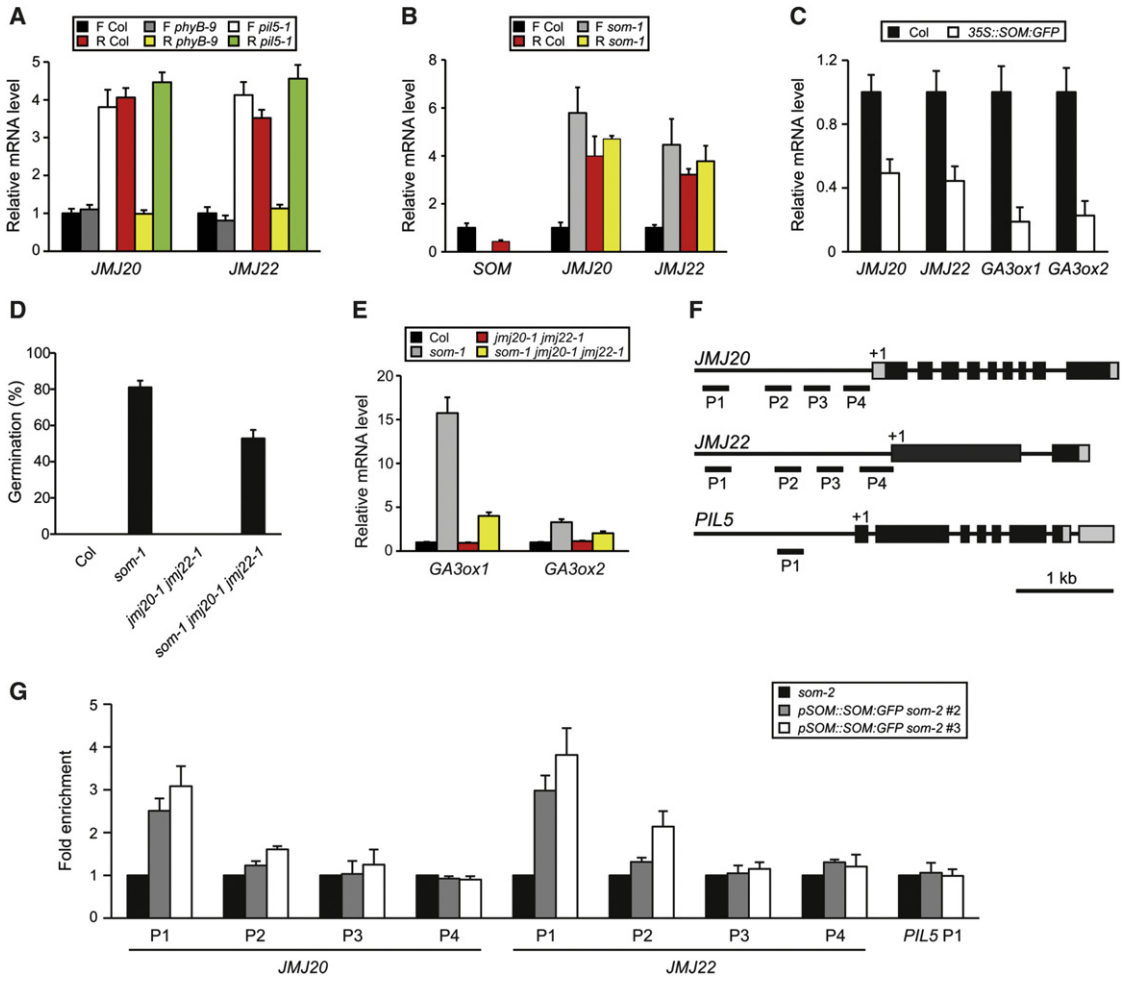

Figure 6. Direct Repression of *JMJ20* and *JMJ22* by SOM

(A and B) qRT-PCR analyses of the transcript levels of *JMJ20*, *JMJ22*, and *SOM* in FR- and R-treated WT, *phyB-9*, *pil5-1*, and *som-1* seeds using gene-specific primers (Supplemental Experimental Procedures). Light treatment was performed as in Figure 3. The levels in F WT were set to 1 after normalization by *ACT2*. Error bars represent SD in (A)–(E) and (G).

(C) qRT-PCR analyses of the transcript levels of *JMJ20*, *JMJ22*, *GA3ox1*, and *GA3ox2* in WT and *35S::SOM:GFP* seeds treated with 5 min of R. The levels in WT were set to 1 after normalization by *ACT2*.

(D) The germination percentage of seeds treated with 5 min of FR. Germinated seeds were counted at 5 days after light treatment.

(E) qRT-PCR analysis of the transcript levels of *GA3ox1* and *GA3ox2* in seeds treated with 5 min of FR. The levels in WT were set to 1 after normalization by *ACT2*.

(F) The gene structures of *JMJ20*, *JMJ22*, and *PIL5*. Schematics are as described in Figure 1A. Regions amplified in ChIP-quantitative PCR (G) are indicated.

(G) The ChIP-quantitative PCR assay with anti-GFP antibody using WT and *pSOM::SOM:GFP* transgenic seeds. Seeds were imbibed for 1 hr, treated with 5 min of FR, and incubated for 12 hr in the dark before harvesting. The P1 region of the *PIL5* promoter served as a nonspecific control. Each region was amplified with locus-specific primers (Supplemental Experimental Procedures). The results are presented as fold enrichment relative to input DNA, and the levels in the nontransgenic control (*som-2*) seeds were set to 1.

See also Figure S4.

by light-independent expression of *JMJ20* or *JMJ22* in seeds. Thus, we studied the phenotype of transgenic plants constitutively expressing *JMJ20* or *JMJ22* (*35S::JMJ20:GFP* or *35S::JMJ22:GFP*; Figure S4D), and found that the light-independent constitutive seed expression of *JMJ20:GFP* or *JMJ22:GFP* alone does not allow the induction of *GA3ox1*/*GA3ox2* mRNAs (Figure S4E), altered H4R3me2s levels at *GA3ox1*/*GA3ox2* (Figure S4G), the binding of JMJ20:GFP or JMJ22:GFP to *GA3ox1*/*GA3ox2* chromatin (Figure S4H), nor an enhanced seed germination phenotype (Figure S4F). Rather, we observed an R-dependent recruitment of constitutively expressed JMJ20:GFP/JMJ22:GFP to *GA3ox1*/*GA3ox2* chromatin (Figure S4H), suggesting that PHYB signaling is required for the association of JMJ20/JMJ22 to *GA3ox1*/*GA3ox2* chromatin as well as for their induction in seeds. Considering the effect of JMJ20/JMJ22 on the R-independent germination of *pil5* and *som* mutants (Figures S4A, 6D, and 6E), the results above suggest that the factor (or signal) allowing JMJ20/JMJ22 recruitment might also be regulated by the PHYB-PIL5-SOM pathway.

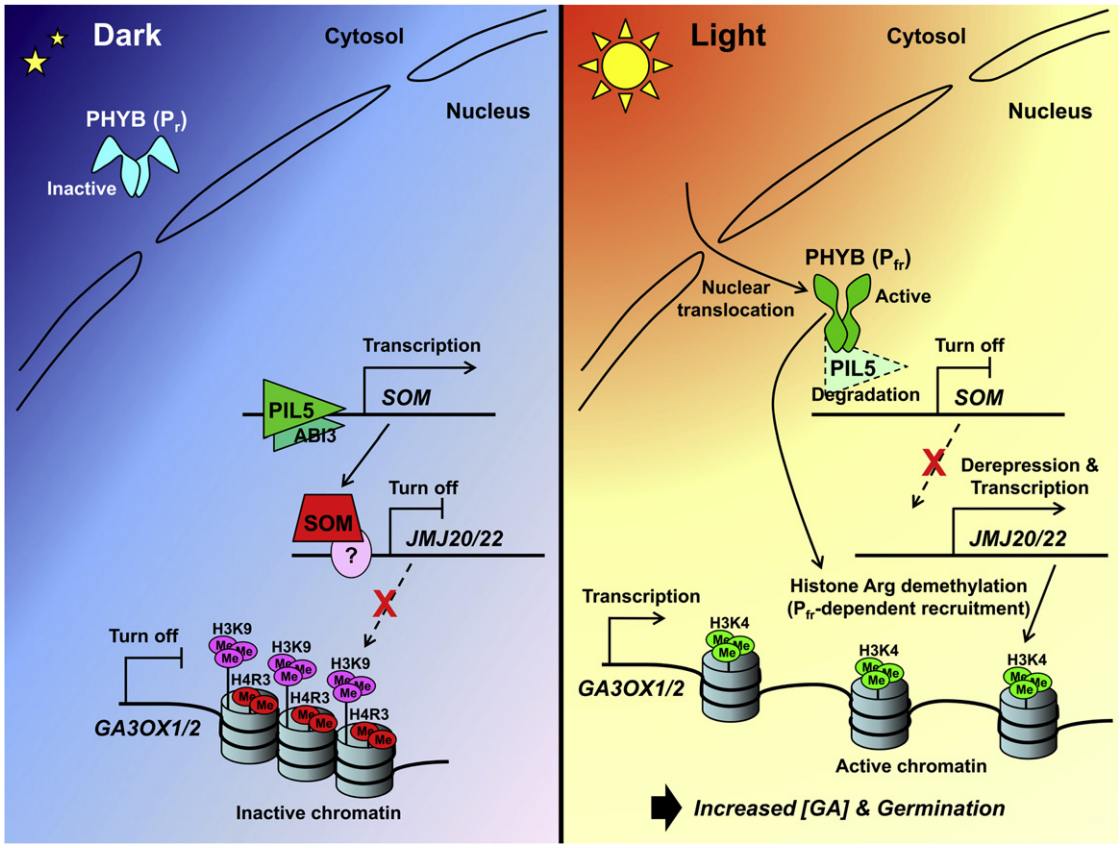

Figure 7. A Proposed Model for the Role of *JMJ20* and *JMJ22* in PHYB-Dependent Seed Germination

The light-activated PHYB-PIL5-SOM pathway allows the induction and targeting of JMJ20/JMJ22 to *GA3ox1/GA3ox2* chromatin. It results in an open chromatin state and active transcription at *GA3ox1/GA3ox2*, which in turn promotes seed germination through increased GA levels. The model does not include the explanation for the nuclear export or import of *SOM* and *JMJ20/JMJ22* mRNAs or proteins, respectively. See the text for details.

A Proposed Model for the Role of JMJ20 and JMJ22 in Light-Dependent Seed Germination

On the basis of our study, we propose a model for the PHYB-dependent seed germination pathway (Figure 7). Under FR or dark conditions, PHYB exists as a cytosol-localized inactive Pr form, which permits PIL5 to accumulate in the nucleus and transcriptionally activate *SOM* in concert with ABI3. The SOM protein in turn directly represses the expression of *JMJ20* and *JMJ22*. When the expression of these HR demethylases is low, repressive H4R3me2s is maintained at high levels on *GA3ox1* and *GA3ox2* chromatin, resulting in low GA levels and no seed germination. However, upon R irradiation, the conversion and translocation of PHYB from the cytosol-localized inactive Pr to the nuclear-localized active Pfr form cause the degradation of the PIL5 protein via the ubiquitin-proteasome system. The depletion of the PIL5 protein leads to the downregulation of *SOM* transcription and the subsequent derepression of *JMJ20* and *JMJ22*. The increased expression and PHYB-dependent recruitment of these functionally redundant HR demethylases to *GA3ox1/GA3ox2* loci induce the expression of *GA3ox1/GA3ox2* by the removal of the repressive H4R3me2s from their chromatin. The increased expression of these GA anabolic genes causes the accumulation of active GA in seeds, which enables embryos to germinate.

DISCUSSION

We report that two *Arabidopsis* JmjC domain-containing proteins, JMJ20 and JMJ22, are HR demethylases that act as positive regulators of seed germination in the PHYB-PIL5-SOM pathway. Their expression was induced by R downstream of SOM, and it directly promoted the induction of GA anabolic genes by reducing repressive H4R3me2s levels after PHYB-dependent recruitment. The role of HR methylation in transcription has been recognized, and a group of catalytic PRMTs has been discovered (reviewed in Di Lorenzo and Bedford, 2011). However, to our knowledge, the dynamic regulation of HR methylation has not been studied in depth because of the lack of discovery of proteins that remove methyl groups from arginine. JMJD6 is the first protein reported to demethylate H3R2 and H4R3 (Chang et al., 2007). However, to our knowledge, the influence of JMJD6 on the level of HR methylation at specific target loci has not been demonstrated. In addition, the biochemical function of JMJD6 as an HR demethylase has been recently challenged (Boeckel et al., 2011; Hong et al., 2010; Webby et al., 2009).

The present study provides strong evidence that the methylation of H4R3 is indeed reversible and that a subgroup of JmjC domain-containing proteins is responsible for it. We found that

the level of H4R3me2s at the promoters of *GA3ox1* and *GA3ox2* is dynamically decreased as seeds in the dark are exposed to R, and this reduction does not occur in *jmj20 jmj22* double mutants. The direct association of JMJ20/JMJ22 with the promoters of *GA3ox1/GA3ox2* and the H4R3me2s/H3R2me2-specific demethylase activity of recombinant JMJ20 for bulk histones strongly support that JMJ20/JMJ22 indeed remove methyl groups from H4R3 at *GA3ox1/GA3ox2*.

How environmental signals influence the epigenetic modification and subsequent transcription of responsive genes is not well understood. Although the detailed mechanism by which JMJ20/JMJ22 demethylate H4R3 at *GA3ox1/GA3ox2* in response to R is not fully understood, we have clearly shown that both the mRNA expression of *JMJ20/JMJ22* and the binding of their proteins to the *GA3ox1/GA3ox2* loci are increased by R through the PHYB-PIL5-SOM pathway. Thus, the R-mediated transcriptional regulation of *JMJ20/JMJ22* and the recruitment of their protein products to target loci could be the underlying basis for the R-induced epigenetic modification and transcriptional activation of *GA3ox1/GA3ox2*. Consistent with a general role for H4R3me2s in gene repression (reviewed in Di Lorenzo and Bedford, 2011), the activation of *GA3ox1/GA3ox2* by R was correlated with the decreased level of H4R3me2s within *GA3ox1/GA3ox2* chromatin. On the other hand, increased levels of H4R3me2s at *GA3ox1/GA3ox2* caused by mutations in *JMJ20/JMJ22* lead to decreased expression of these GA anabolic genes.

It is not yet clear how H4R3me2s contributes to gene repression. H4R3me2s might influence the generation of other histone markers such as lysine methylation, or serve as a binding site for repressive effectors. Notably, it was recently reported that H4R3me2s provides a direct binding site for the DNA methyltransferase DNMT3A at the human *β-globin* locus (Zhao et al., 2009). The loss of H4R3me2s by knockdown of PRMT5 resulted in a loss of DNA methylation (DNAme) and gene activation. In this regard, it would be of interest to test whether a parallel event occurs at *GA3ox1/GA3ox2* in *Arabidopsis*. Interestingly, in *jmj20 jmj22*, the levels of another repressive histone marker, H3K9me3, were increased at *GA3ox1/GA3ox2*, whereas the levels of H3K27me3 were not. Considering crosstalk between DNAme and H3K9me (e.g., Johnson et al., 2007; Jackson et al., 2002), it is possible that the increased H3K9me3 in *jmj20 jmj22* mutants might be a consequence of increased DNAme that was caused by the increased H4R3me2s. It was reported that a long-term cold treatment known as vernalization increases H4R3me2s together with H3K9me3 and H3K27me3 at *FLC* in an AtPRMT5-dependent manner (Schmitz et al., 2008). Thus, H4R3me2s is necessary for H3K9me3 and H3K27me3 at *FLC* during vernalization. However, the fact that DNAme is not induced at *FLC* during vernalization (Jean Finnegan et al., 2005) suggests a possibility that DNAme might not necessarily be included in the crosstalk between these repressive markers. Comparing DNAme levels between *jmj20 jmj22* and WT or before and after R treatment at *GA3ox1/GA3ox2* might be a way to address the question of crosstalk between HR methylation, histone lysine methylation, and DNAme.

During light-induced seed germination, the PHYB-PIL5-mediated light signal regulates the GA and ABA metabolic genes partly through SOM (Kim et al., 2008). However, how SOM regulates these metabolic genes was not clear (Kim et al., 2008), and thus the identification of the downstream components of SOM was necessary to fully understand signaling of light-mediated seed germination. Our study reveals the link between SOM and GA anabolic genes (*GA3ox1/GA3ox2*) by demonstrating that *JMJ20/JMJ22* are two of the direct repressive targets of the SOM protein and that the JMJ20/JMJ22 proteins in turn directly target *GA3ox1/GA3ox2* for activation. The complexity of the regulation of light-induced seed germination is revealed by the fact that JMJ20/JMJ22 do not control all of the genes affected by SOM in addition to the fact that SOM itself also regulates a part of the downstream genes of PIL5 (Oh et al., 2009; Kim et al., 2008). Thus, the initial light signal must be amplified and transduced through multiple layers of signaling to ensure proper control of the complicated downstream physiological changes that are collectively required for the transition from seed dormancy to vegetative development.

The *GA3ox1/GA3ox2*-specific alteration in expression by the *jmj20 jmj22* mutations suggests that JMJ20/JMJ22 should have target specificity. Because JMJ20/JMJ22 contain none of the known DNA-binding or histone marker-binding domains, they might be guided to specific loci by other target-discriminating factors in an R-dependent manner. Such factors, which, to our knowledge, are yet to be discovered, should also be positive regulators of *GA3ox1/GA3ox2* during seed germination. In this regard, studies on JMJ20/JMJ22-containing protein complexes and their activity control by light might be important future tasks for the elucidation of detailed germination-control mechanisms.

Our study shows that epigenetic derepression during seed germination is an important control process at *GA3ox1/GA3ox2*. Because germination is the final stage of release from dormancy, establishing and maintaining dormancy appear to involve repressive epigenetic mechanisms at these loci. Therefore, it will be an important future task to understand the role of repressive epigenetic mechanisms and to identify key epigenetic regulatory components acting at these loci during dormancy. In this regard, the enrichment of H4R3me2s and H3K9me3 at the loci before the light signal suggests that at least some PRMTs and H3K9 methyltransferases play roles in chromatin repression during dormancy. The identification of epigenetically controlled targets, other than *GA3ox1/GA3ox2*, will be another interesting future task.

EXPERIMENTAL PROCEDURES

Plant Materials and Growth Conditions

The *jmj20-1* and *jmj22-1* mutants are in the Columbia-0 (Col; WT) background and were obtained from the SAIL (SAIL_680_G02) and SALK (SALK_146176) collections, respectively. The *som-1*, *som-2*, *phyB-9*, *pil5-1* mutants, and the *35S::SOM:GFP* transgenic plants are in the Col background. Plants were grown under 100 μmol m^{-2} s^{-1} cool white fluorescent lights with a 16 hr light and 8 hr dark photoperiod (LD) at 22°C.

Germination Assay

Seeds used in the germination assays were harvested from plants grown side by side in the same tray, and the harvested seeds were dried for more than 2 months at room temperature. For the PHYB-dependent germination assay, seeds were sown on one-tenth strength MS media without sucrose and imbibed at 22°C for 1 hr in the dark. Then, they were exposed to 1 μmol m^{-2} s^{-1} of FR for 5 min, and 20 μmol m^{-2} s^{-1} of R was immediately

irradiated for 5 min unless specified otherwise. Germinated seeds were counted by the emergence of the radicle. At least 80–120 seeds were used for one set, and triplicate sets were analyzed for statistical assessment.

Gene Expression Analysis

Total RNA was extracted from imbibed seeds as previously described (Suzuki et al., 2004) with minor modifications, and the details of qRT-PCR analyses are provided in the Supplemental Experimental Procedures.

ChIP Assay

Chromatin isolation from imbibed seeds was performed as previously described (Oh et al., 2007), and the details of ChIP assays are provided in the Supplemental Experimental Procedures.

Histochemical GUS Assay

A genomic fragment containing the 1.5 kb promoter and the entire coding region of *JMJ20* was amplified from WT DNA and cloned into the pMDC163 gateway binary vector, resulting in the *JMJ20:GUS* construct. To generate the *JMJ22:GUS* construct, a genomic region spanning the 1 kb promoter and the full-length coding sequence of *JMJ22* was amplified from WT DNA and cloned into pPZP211-GUS (Noh and Amasino, 2003). The *JMJ20:GUS* and *JMJ22:GUS* constructs were introduced into *jmj20-1 jmj22-1* double mutants via *Agrobacterium*-mediated transformation by the floral dip method (Clough and Bent, 1998). One-hour-imbibed transgenic seeds were treated with FR and R and kept in the dark for 12 hr. Then, the seeds were fixed with 90% acetone on ice for 30 min under a green safe light and were washed twice with KPO_4 buffer. The fixed seeds were dissected, and the exposed embryos were stained for GUS activity at 37°C for 3 hr, as described previously (Schomburg et al., 2001). The GUS expression pattern was analyzed as described (Hong et al., 2009).

Subcellular Localization Study

A genomic coding region of *JMJ20* was PCR amplified from WT DNA and introduced into the pEarleygate103 gateway binary vector, resulting in the *35S::JMJ20:GFP* construct. To generate the *35S::JMJ22:GFP* construct, a *JMJ22* cDNA fragment was PCR amplified from a WT cDNA pool and cloned into the JJ461 binary vector (Han et al., 2007). Both GFP fusion constructs were transformed into WT plants via *Agrobacterium*-mediated transformation using the floral dip method (Clough and Bent, 1998). Root epidermal cells from 10-day-old LD-grown transgenic seedlings were observed using the DE/LSM510 NLO multiphoton confocal laser scanning microscope (Carl Zeiss). DAPI was used to stain nuclei. Merged images were obtained using LSM image browser software.

Nuclear fractionation was performed as previously described with minor modifications (Kinkema et al., 2000). Briefly, about 0.2 g of seed tissue was ground in liquid nitrogen, resuspended in Honda buffer (2.5% Ficoll 400, 5% dextran T40, 0.4 M sucrose, 25 mM Tris-HCl [pH 7.4], 10 mM $MgCl_2$, 10 mM β-mercaptoethanol, proteinase inhibitor cocktail), and filtered through Miracloth (Calbiochem). Triton X-100 was added to a final concentration of 0.5%, and the mixture was incubated on ice for 15 min. The solution was centrifuged at 1,500 × *g* for 5 min, and the supernatant was used as nonnuclear fraction. The pellet was washed with Honda buffer and centrifuged to pellet nuclei. Antibodies used in the western blot analyses were as follows: α-GUS (Invitrogen; A5790), α-H3 (Abcam; ab1791), and α-tubulin (Sigma-Aldrich; T9026).

In Vitro Histone Demethylase Assay

JMJ20:6×His was expressed in *E. coli* BL21(DE3) at 18°C for 16 hr with 1 mM isopropyl β-D-1-thiogalactopyranoside. Cells were harvested in a resuspension buffer (50 mM Tris-HCl [pH 8.0], 500 mM NaCl, 5% glycerol, 0.3 mM phenylmethyl sulfonyl fluoride) and lysed by sonication. Cell debris was removed by centrifugation, and the supernatant was incubated with Ni-NTA agarose beads (QIAGEN) with 20 mM imidazole for 2 hr at 4°C. The beads were washed with the resuspension buffer, wash buffer A (50 mM Tris-HCl [pH 8.0], 1 M NaCl, 5% glycerol), and wash buffer B (50 mM Tris-HCl [pH 8.0], 300 mM NaCl, 5% glycerol). JMJ20:6×His was eluted with elution buffer (50 mM Tris-HCl [pH 8.0], 300 mM NaCl, 5% glycerol, 100 mM imidazole). Histone demethylase assay using purified JMJ20:6×His is described in detail in the Supplemental Experimental Procedures.

SUPPLEMENTAL INFORMATION

Supplemental Information includes four figures and Supplemental Experimental Procedures and can be found with this article online at doi:10.1016/j.devcel.2012.01.024.

ACKNOWLEDGMENTS

We thank Giltsu Choi for providing *som-1*, *som-2*, *pSOM::SOM:GFP*, and *35S::SOM:GFP* plants. This work was supported by the National Research Foundation (NRF; 2011-0015177) and by the Next-Generation BioGreen21 Program (TAGC and SSAC) of the Rural Development Administration. B.N. was also supported by a grant from the NRF (2010-359-C00032). J.-N.C. was supported by the BK21 Program. J.-J.S. was supported by the WCU program (R31-2008-000-10071-0). Work in R.M.A.'s group was supported by the University of Wisconsin and the National Institutes of Health (1R01GM079525).

Received: March 22, 2011
Revised: January 6, 2012
Accepted: January 31, 2012
Published online: April 5, 2012

REFERENCES

Boeckel, J.N., Guarani, V., Koyanagi, M., Roexe, T., Lengeling, A., Schermuly, R.T., Gellert, P., Braun, T., Zeiher, A., and Dimmeler, S. (2011). Jumonji domain-containing protein 6 (Jmjd6) is required for angiogenic sprouting and regulates splicing of VEGF-receptor 1. Proc. Natl. Acad. Sci. USA *108*, 3276–3281.

Borthwick, H.A., Hendricks, S.B., Parker, M.W., Toole, E.H., and Toole, V.K. (1952). A reversible photoreaction controlling seed germination. Proc. Natl. Acad. Sci. USA *38*, 662–666.

Chang, B., Chen, Y., Zhao, Y., and Bruick, R.K. (2007). JMJD6 is a histone arginine demethylase. Science *318*, 444–447.

Clough, S.J., and Bent, A.F. (1998). Floral dip: a simplified method for *Agrobacterium*-mediated transformation of *Arabidopsis thaliana*. Plant J. *16*, 735–743.

Di Lorenzo, A., and Bedford, M.T. (2011). Histone arginine methylation. FEBS Lett. *585*, 2024–2031.

Fischle, W., Wang, Y., and Allis, C.D. (2003). Histone and chromatin cross-talk. Curr. Opin. Cell Biol. *15*, 172–183.

Gabriele, S., Rizza, A., Martone, J., Circelli, P., Costantino, P., and Vittorioso, P. (2010). The Dof protein DAG1 mediates PIL5 activity on seed germination by negatively regulating GA biosynthetic gene *AtGA3ox1*. Plant J. *61*, 312–323.

Guccione, E., Bassi, C., Casadio, F., Martinato, F., Cesaroni, M., Schuchlautz, H., Lüscher, B., and Amati, B. (2007). Methylation of histone H3R2 by PRMT6 and H3K4 by an MLL complex are mutually exclusive. Nature *449*, 933–937.

Hahn, P., Böse, J., Edler, S., and Lengeling, A. (2008). Genomic structure and expression of Jmjd6 and evolutionary analysis in the context of related JmjC domain containing proteins. BMC Genomics *9*, 293.

Han, S.K., Song, J.D., Noh, Y.S., and Noh, B. (2007). Role of plant CBP/p300-like genes in the regulation of flowering time. Plant J. *49*, 103–114.

Hong, E.H., Jeong, Y.M., Ryu, J.Y., Amasino, R.M., Noh, B., and Noh, Y.S. (2009). Temporal and spatial expression patterns of nine *Arabidopsis* genes encoding Jumonji C-domain proteins. Mol. Cells *27*, 481–490.

Hong, X., Zang, J., White, J., Wang, C., Pan, C.-H., Zhao, R., Murphy, R.C., Dai, S., Henson, P., Kappler, J.W., et al. (2010). Interaction of JMJD6 with single-stranded RNA. Proc. Natl. Acad. Sci. USA *107*, 14568–14572.

Hyllus, D., Stein, C., Schnabel, K., Schiltz, E., Imhof, A., Dou, Y., Hsieh, J., and Bauer, U.M. (2007). PRMT6-mediated methylation of R2 in histone H3 antagonizes H3 K4 trimethylation. Genes Dev. *21*, 3369–3380.

Jackson, J.P., Lindroth, A.M., Cao, X., and Jacobsen, S.E. (2002). Control of CpNpG DNA methylation by the KRYPTONITE histone H3 methyltransferase. Nature *416*, 556–560.

Jean Finnegan, E., Kovac, K.A., Jaligot, E., Sheldon, C.C., James Peacock, W., and Dennis, E.S. (2005). The downregulation of *FLOWERING LOCUS C* (*FLC*) expression in plants with low levels of DNA methylation and by vernalization occurs by distinct mechanisms. Plant J. *44*, 420–432.

Jeong, J.H., Song, H.R., Ko, J.H., Jeong, Y.M., Kwon, Y.E., Seol, J.H., Amasino, R.M., Noh, B., and Noh, Y.S. (2009). Repression of *FLOWERING LOCUS T* chromatin by functionally redundant histone H3 lysine 4 demethylases in *Arabidopsis*. PLoS ONE *4*, e8033.

Johnson, L.M., Bostick, M., Zhang, X., Kraft, E., Henderson, I., Callis, J., and Jacobsen, S.E. (2007). The SRA methyl-cytosine-binding domain links DNA and histone methylation. Curr. Biol. *17*, 379–384.

Kim, D.H., Yamaguchi, S., Lim, S., Oh, E., Park, J., Hanada, A., Kamiya, Y., and Choi, G. (2008). SOMNUS, a CCCH-type zinc finger protein in *Arabidopsis*, negatively regulates light-dependent seed germination downstream of PIL5. Plant Cell *20*, 1260–1277.

Kinkema, M., Fan, W., and Dong, X. (2000). Nuclear localization of NPR1 is required for activation of *PR* gene expression. Plant Cell *12*, 2339–2350.

Ko, J.H., Mitina, I., Tamada, Y., Hyun, Y., Choi, Y., Amasino, R.M., Noh, B., and Noh, Y.S. (2010). Growth habit determination by the balance of histone methylation activities in *Arabidopsis*. EMBO J. *29*, 3208–3215.

Koornneef, M., Bentsink, L., and Hilhorst, H. (2002). Seed dormancy and germination. Curr. Opin. Plant Biol. *5*, 33–36.

Kouzarides, T. (2007). Chromatin modifications and their function. Cell *128*, 693–705.

Li, B., Carey, M., and Workman, J.L. (2007). The role of chromatin during transcription. Cell *128*, 707–719.

Mazzella, M.A., Arana, M.V., Staneloni, R.J., Perelman, S., Rodriguez Batiller, M.J., Muschietti, J., Cerdán, P.D., Chen, K., Sánchez, R.A., Zhu, T., et al. (2005). Phytochrome control of the *Arabidopsis* transcriptome anticipates seedling exposure to light. Plant Cell *17*, 2507–2516.

Noh, Y.S., and Amasino, R.M. (2003). PIE1, an ISWI family gene, is required for *FLC* activation and floral repression in *Arabidopsis*. Plant Cell *15*, 1671–1682.

Ogawa, M., Hanada, A., Yamauchi, Y., Kuwahara, A., Kamiya, Y., and Yamaguchi, S. (2003). Gibberellin biosynthesis and response during *Arabidopsis* seed germination. Plant Cell *15*, 1591–1604.

Oh, E., Kim, J., Park, E., Kim, J.I., Kang, C., and Choi, G. (2004). PIL5, a phytochrome-interacting basic helix-loop-helix protein, is a key negative regulator of seed germination in *Arabidopsis thaliana*. Plant Cell *16*, 3045–3058.

Oh, E., Yamaguchi, S., Kamiya, Y., Bae, G., Chung, W.I., and Choi, G. (2006). Light activates the degradation of PIL5 protein to promote seed germination through gibberellin in *Arabidopsis*. Plant J. *47*, 124–139.

Oh, E., Yamaguchi, S., Hu, J., Yusuke, J., Jung, B., Paik, I., Lee, H.S., Sun, T.P., Kamiya, Y., and Choi, G. (2007). PIL5, a phytochrome-interacting bHLH protein, regulates gibberellin responsiveness by binding directly to the GAI and RGA promoters in *Arabidopsis* seeds. Plant Cell *19*, 1192–1208.

Oh, E., Kang, H., Yamaguchi, S., Park, J., Lee, D., Kamiya, Y., and Choi, G. (2009). Genome-wide analysis of genes targeted by PHYTOCHROME INTERACTING FACTOR 3-LIKE5 during seed germination in *Arabidopsis*. Plant Cell *21*, 403–419.

Park, J., Lee, N., Kim, W., Lim, S., and Choi, G. (2011). ABI3 and PIL5 collaboratively activate the expression of *SOMNUS* by directly binding to its promoter in imbibed *Arabidopsis* seeds. Plant Cell *23*, 1404–1415.

Pedersen, M.T., and Helin, K. (2010). Histone demethylases in development and disease. Trends Cell Biol. *20*, 662–671.

Schmitz, R.J., Sung, S., and Amasino, R.M. (2008). Histone arginine methylation is required for vernalization-induced epigenetic silencing of *FLC* in winter-annual *Arabidopsis thaliana*. Proc. Natl. Acad. Sci. USA *105*, 411–416.

Schomburg, F.M., Patton, D.A., Meinke, D.W., and Amasino, R.M. (2001). *FPA*, a gene involved in floral induction in *Arabidopsis*, encodes a protein containing RNA-recognition motifs. Plant Cell *13*, 1427–1436.

Seo, M., Hanada, A., Kuwahara, A., Endo, A., Okamoto, M., Yamauchi, Y., North, H., Marion-Poll, A., Sun, T.P., Koshiba, T., et al. (2006). Regulation of hormone metabolism in *Arabidopsis* seeds: phytochrome regulation of abscisic acid metabolism and abscisic acid regulation of gibberellin metabolism. Plant J. *48*, 354–366.

Seo, M., Nambara, E., Choi, G., and Yamaguchi, S. (2009). Interaction of light and hormone signals in germinating seeds. Plant Mol. Biol. *69*, 463–472.

Shinomura, T., Nagatani, A., Chory, J., and Furuya, M. (1994). The induction of seed germination in *Arabidopsis thaliana* is regulated principally by phytochrome B and secondarily by phytochrome A. Plant Physiol. *104*, 363–371.

Suzuki, Y., Kawazu, T., and Koyama, H. (2004). RNA isolation from siliques, dry seeds, and other tissues of *Arabidopsis thaliana*. Biotechniques *37*, 542.

Toyomasu, T., Kawaide, H., Mitsuhashi, W., Inoue, Y., and Kamiya, Y. (1998). Phytochrome regulates gibberellin biosynthesis during germination of photoblastic lettuce seeds. Plant Physiol. *118*, 1517–1523.

Webby, C.J., Wolf, A., Gromak, N., Dreger, M., Kramer, H., Kessler, B., Nielsen, M.L., Schmitz, C., Butler, D.S., Yates, J.R., 3rd., et al. (2009). Jmjd6 catalyses lysyl-hydroxylation of U2AF65, a protein associated with RNA splicing. Science *325*, 90–93.

Williams, J., Phillips, A.L., Gaskin, P., and Hedden, P. (1998). Function and substrate specificity of the gibberellin 3beta-hydroxylase encoded by the *Arabidopsis GA4* gene. Plant Physiol. *117*, 559–563.

Yamaguchi, S., Smith, M.W., Brown, R.G., Kamiya, Y., and Sun, T. (1998). Phytochrome regulation and differential expression of gibberellin 3beta-hydroxylase genes in germinating *Arabidopsis* seeds. Plant Cell *10*, 2115–2126.

Yamauchi, Y., Takeda-Kamiya, N., Hanada, A., Ogawa, M., Kuwahara, A., Seo, M., Kamiya, Y., and Yamaguchi, S. (2007). Contribution of gibberellin deactivation by AtGA2ox2 to the suppression of germination of dark-imbibed *Arabidopsis thaliana* seeds. Plant Cell Physiol. *48*, 555–561.

Zhao, Q., Rank, G., Tan, Y.T., Li, H., Moritz, R.L., Simpson, R.J., Cerruti, L., Curtis, D.J., Patel, D.J., Allis, C.D., et al. (2009). PRMT5-mediated methylation of histone H4R3 recruits DNMT3A, coupling histone and DNA methylation in gene silencing. Nat. Struct. Mol. Biol. *16*, 304–311.